

# Effect of warm working on the precipitation of vanadium carbide in a medium carbon austenitic steel

S. J. HARRIS, N. R. NAG\*

*Department of Metallurgy and Materials Science, University of Nottingham, UK*

Electrical resistance measurements and electron microscope observations have been used to interpret the ageing characteristics of a 0.4% carbon–24% manganese–0.7% vanadium steel in the temperature range 550 to 700°C. It has been shown that vanadium carbides form in a diffusion controlled process, activation energy 295 kJ mol<sup>-1</sup>, producing precipitate densities in the matrix of  $\sim 10^{16}$  cm<sup>-3</sup>. The kinetics suggest that nucleation depends on the existence of critical sized substitutional solute atom-vacancy clusters and that once the incubation period has elapsed the nucleation rate falls rapidly and beyond 0.1 fraction transformed further reaction takes place by growth only. Increasing amounts of deformation at the ageing temperature reduces the incubation period and total reaction time, progressively. The relevance of these results to help explain the ausforming behaviour of low alloy steel is stressed.

## 1. Introduction

The effect of “warm” deformation on the properties of low alloy steels has been demonstrated many times in the so-called “ausforming” process. Many workers [1–4] have put forward ideas to explain the increase in strength (without the resultant loss in ductility) resulting in these steels after the sequence: austenitize (> 850°C)—warm work (50 to 70% RA in temperature range 525 to 625°C)—cool to form a martensitic structure—temper in range 150 to 650°C. Such theories include reduction in austenitic grain size and, therefore, martensite plate size, alteration of martensitic sub-structure, and precipitation hardening effects. In low alloy steels, i.e. those containing less than 6% total alloying content (chromium, nickel, manganese, etc.) it has proved difficult to study the processes which take place during the warm working of “metastable” austenite, since examination has to take place at the working temperature. Cooling down to room temperature allows the martensitic reaction to take place, which introduces significant changes in microstructures that

mask any evidence of precipitation or substructure produced during working.

The present study attempts to examine the morphology and kinetics of carbide precipitation in a medium carbon steel with a single carbon forming element present i.e. 0.7% vanadium. Such a composition relates to a low alloy steel that has been shown [2, 3] to be responsive to ausforming. However, to make such a study possible a relatively large amount of manganese (25%) has been added to stabilize the austenite down to room temperature and thus prevent a martensitic reaction. Since mechanical working is an integral part of the ausforming process the effect of deformation on the kinetics of carbide precipitation is considered to be relevant.

## 2. Experimental

The steel was induction-vacuum melted and supplied in the form of 16 mm diameter rod or 9.5 mm thick 50 mm wide plate. Chemical analysis of the material examined is shown in Table I.

Kinetics have been determined using a measure-

\*Present address: British Steel Corporation (Strip Mills Division), Port Talbot, UK.

TABLE I Chemical analysis of steel

Element	wt %	Element	wt %
C	0.40	P	0.003
Si	0.04	Mo	0.01
Mn	24.60	V	0.68
S	0.014		

ment of the change of electrical resistance during isothermal ageing in the temperature range 550 to 700°C. Details of the technique used for resistance measurement have been described elsewhere [5]. Prior to ageing the steels were solution treated at 1200°C in vacuo and then quenched in 10% brine solution.  $R_t$ , the resistance of a sample after an interval of time  $t$  at the ageing temperature, and  $R_0$  the resistance at zero time, were measured, allowing the change of resistance

$$\frac{\Delta R}{R_0} = \left( \frac{R_t - R_0}{R_0} \right)$$

to be plotted as a percentage against  $\log t$ . For the series of samples subjected to plastic deformation prior to ageing a dead weight load was applied with the aid of a modified creep machine. The amount of deformation was measured as the percentage elongation of the sample.

Electron microscopy has been carried out on separate samples; these were obtained from 0.25 mm thick strip (20 mm × 10 mm in size) that had been heat-treated in evacuated silica capsules. Initially, the 0.25 mm strip thickness had been obtained by alternate cold rolling and annealing of the supplied 9.5 mm thick plate material. A solution treatment temperature of 1200°C for 1h was used. Specimens were either directly aged in a salt bath or quenched in a 10% brine solution at room temperature by breaking the capsule,

followed by re-encapsulation under vacuum in a silica tube and reheating to age at higher temperatures. Thin foils were prepared from the heat-treated samples by electropolishing first in a 95:5 acetic-perchloric acid mixture using a flat stainless steel cathode at a voltage of 39V and a temperature of ~25°C. Final polishing was then carried out in an electrolyte containing 3% solution of perchloric acid in methanol at a temperature below 70°C. Manganese base austenitic steels are susceptible to rapid corrosion and oxidation and for this reason foils were examined in the microscope immediately after preparation.

### 3. Experimental results

#### 3.1. Electrical resistance changes

The resistance values measured during ageing in the temperature range 550 to 700°C were normalized and are plotted in Fig. 1. All curves showed an initial time (incubation period) for which there was no detectable change of resistance, this being followed by a gradual decrease of resistance with time at a very slow rate. This incubation period increased with decreasing ageing temperature. Complete curves have been obtained at temperatures 675 and 700°C; the curve at 700°C tailed off after 300h whereas this stage has been reached at 675°C in 1300h.

The effect of deformation introduced into samples prior to ageing at 675°C on the normalized resistance-time curve is shown in Fig. 2. Two deformation levels, 5 and 10%, were employed. The incubation period, the total resistance drop and the time for the reaction to reach completion decreased with increasing deformation. The imposition of 10% deformation reduces the incubation period from 7h (straight ageing) to

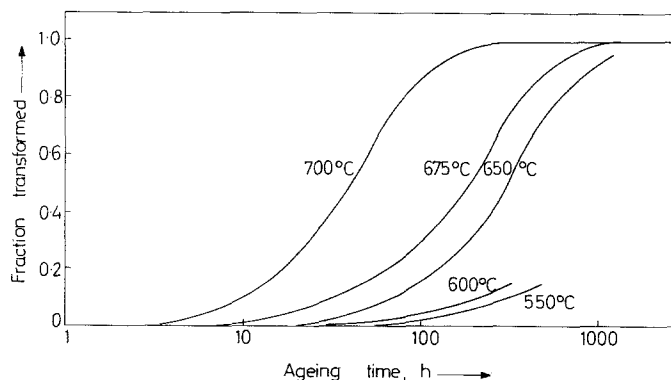


Figure 1 Normalized ageing curves obtained from electrical resistance measurements on brine-quenched samples of the Mn-V-C steel.

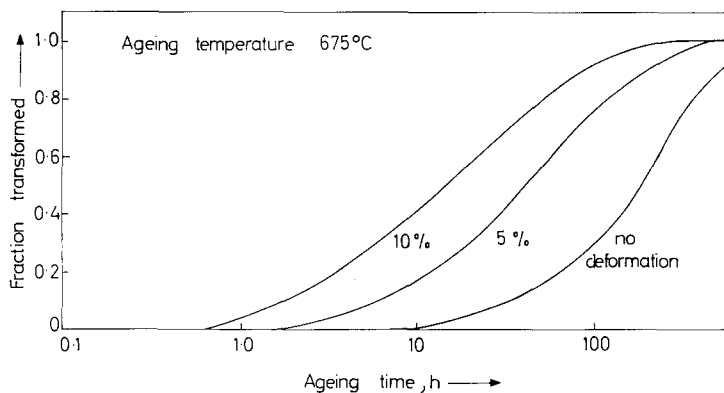


Figure 2 The effect of prior mechanical deformation on the ageing characteristics of the Mn-V-C steel at 675°C.

0.7h and the reaction completion time from 1300 to 300h. Assuming that the total resistance drop represented the total fraction of solute precipitated, the straight ageing curves and deformed and aged curves at 675°C were analysed in terms of the Johnson-Mehl equation:

$$y = 1 - \exp(-kt)^n \quad (1)$$

where  $y$  is the fraction precipitated in time  $t$ ;  $k$ , the rate constant and  $n$ , a constant which can be

used to interpret the reaction kinetics. Figs. 3 and 4 show plots of  $\log \log (1/1-y)$  versus  $\log t$  derived from the straight aged and deformed and aged curves respectively. Values of  $n$  which were measured from the slopes of straight lines of Fig. 3 and 4 are shown in Table II. A change in slope was noted at each ageing temperature (except 550°C) in the neighbourhood of 0.1 fraction transformed. An activation energy of 295 kJ mol<sup>-1</sup> (70.5 kcal) was determined from an Arrhenius

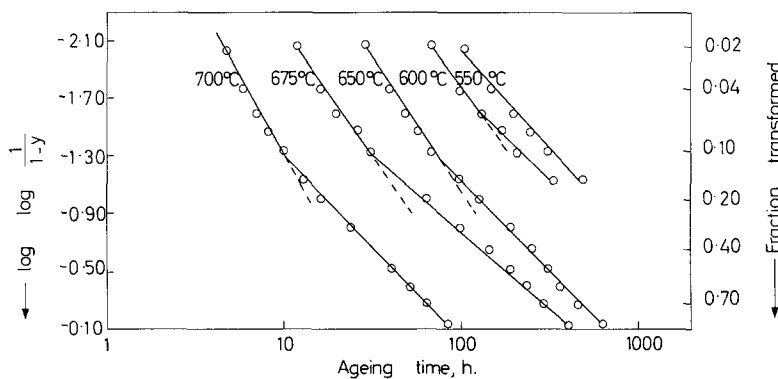


Figure 3 Use of the Johnson-Mehl equation to analyse the ageing curves shown in Fig. 1.

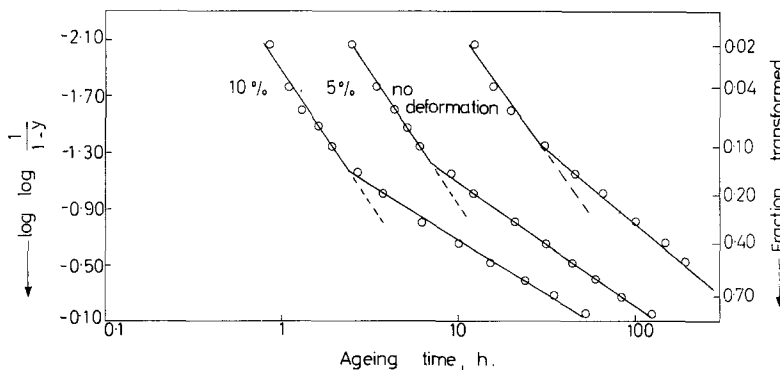


Figure 4 Johnson-Mehl analysis of deformed and aged curves (675°C) shown in Fig. 2.

TABLE II Values of Johnson–Mehl time exponent,  $n$ 

Temperature (°C)	% deformation	Time exponent, $n$	
		$y < 0.1$	$y > 0.1$
550	0	1.3	1.3
600	0	1.8	1.1
650	0	1.9	1.1
675	0	1.8	1.1
	5	1.8	0.9
	10	2.1	0.8
700	0	2.2	1.3

type plot for the precipitation process during straight ageing and this value was found to be constant at all stages of precipitation.

### 3.2. Electron microscopy

#### 3.2.1. As-quenched condition

The as-quenched structure (see Fig. 5) shows little evidence of undissolved particles, thus in-



Figure 5 Transmission electron micrograph of Mn–V–C steel after solution treatment (1200°C) and brine-quenching.  $\times 16\,500$ .

dicating that the majority of the vanadium carbide had gone into solution during treatment at 1200°C. Some of the quenched-in dislocations were in the form of stacking fault nodes, indicating that the material had a low stacking fault energy.

#### 3.2.2. Ageing at 650°C

Fig. 6 shows the microstructural changes which took place during ageing at 650°C for various times. After 10h ageing there was basically no change in the dislocation structure from that of as-quenched structures. A high density of

what was interpreted as precipitates appeared in samples aged for 40h (see Fig. 6a); at this stage ( $y = 0.04$ ) only strain contrast effects could be detected. However, taking the length of lines of no contrast as an approximate indication of the diameter of the particle, the maximum size of the particle was  $\sim 50$  Å. If it is assumed that the thickness of the foil is  $\sim 1500$  Å the density of precipitates was estimated at  $10^{12}$  cm $^{-3}$ . Diffraction patterns at this stage showed only matrix spots.

The number of particles which could be detected from their strain contrast after 80h of ageing ( $y = 0.12$ ) was estimated to be  $\sim 10^{15}$  cm $^{-3}$  (Fig. 6b). Diffraction patterns (see Fig. 6c) at this stage showed the presence of precipitate spots. The “ $d$ ” spacings of the precipitate spots were measured and the precipitates were identified as vanadium carbide.

Structure after 360h ( $y = 0.6$ ) ageing at 650°C is shown in Fig. 6e. Most of the particles had grown to a larger size ( $\sim 400$  Å) but some of the particles still showed strain contrast. The density of the particles at this stage could not be calculated due to image overlap.

#### 3.2.3. Ageing at 700°C

Ageing at 700°C of brine quenched specimens for 35h ( $y = 0.45$ ) gave a combination of matrix and stacking fault precipitates. The matrix particle sizes were  $\sim 500$  Å in diameter. No strain contrast was detected and a number of particles had a tendency to form on undissociated dislocation lines. Density of the particles was about  $10^{10}$  cm $^{-3}$  (see Fig. 7).

#### 3.2.4. Direct ageing

Direct ageing (i.e. quenching from solution treatment temperature to the ageing temperature) was carried out on a series of samples at 725, 700 and 680°C. No matrix precipitates were observed after ageing at 725 and 700°C; precipitation had taken place on grain boundaries and dislocations. Direct ageing at 680°C for 70h showed matrix as well as stacking fault precipitation (see Fig. 8a). So in the present alloy it appears that a critical temperature for matrix precipitation lies between 680 and 700°C. In order to examine directly the effect of quenching to room temperature prior to ageing on the density of matrix precipitation, another specimen was quenched in 10% brine from the solution treatment tempera-

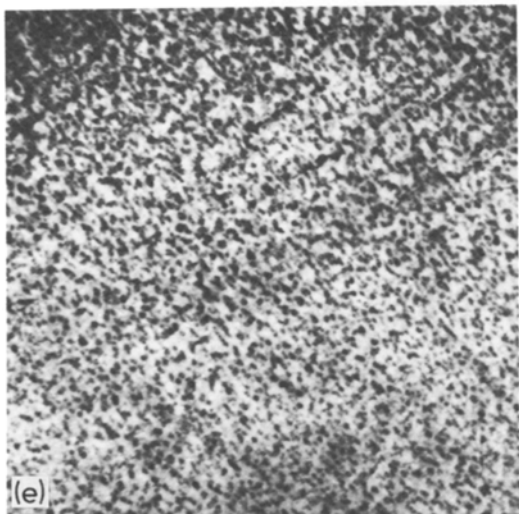
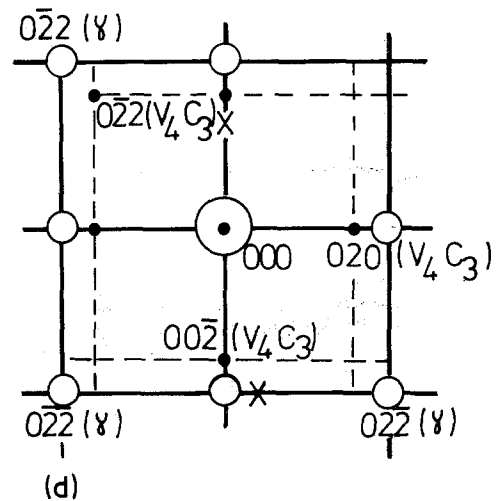
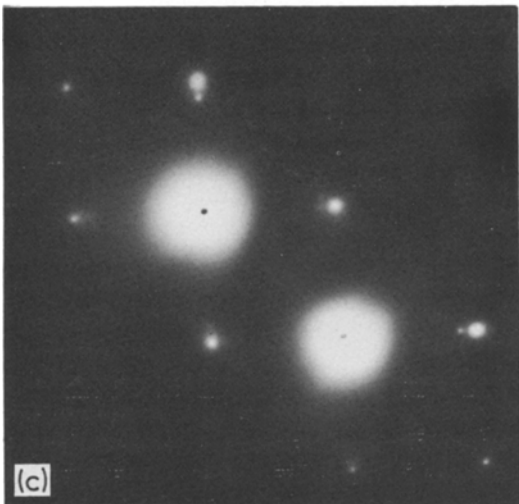
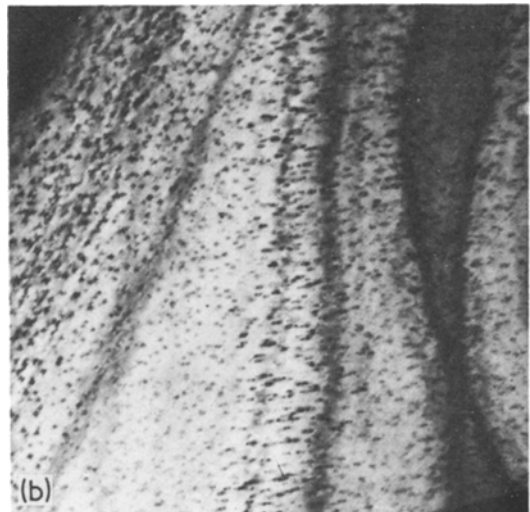
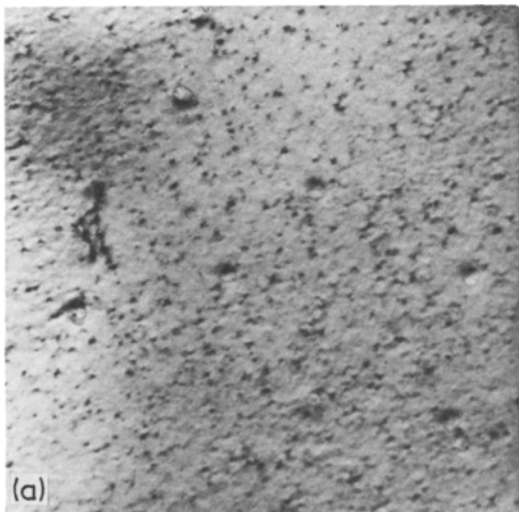


Figure 6 Electron micrographs of the Mn-V-C steel after ageing solution treated and brine-quenched samples for various periods at 650°C; (a) 40 h,  $\times 72\,000$ , (b) 80 h,  $\times 72\,000$ , (c) selected-area diffraction pattern of the area shown in (b), foil orientation  $\{100\}$  (d) diffraction pattern of (c), (e) 360 h,  $\times 50\,000$ . Key for (d):  $\circ$ , Matrix spot (b);  $\bullet$ , precipitate spot ( $V_4C_3$ ); X, double diffraction spot.

ture and aged at 680°C for 70h. The result is shown in Fig. 8b. Matrix precipitates were observed at a higher density than those observed in Fig. 8a and no evidence of stacking fault formation was obtained. The density of the matrix precipitates in the brine quenched and aged specimen was twice the level of that measured on the directly aged one, see Table III.

### 3.2.5. Step ageing

Since the water-quenched-and-aged specimens, but not the directly aged specimens, showed matrix

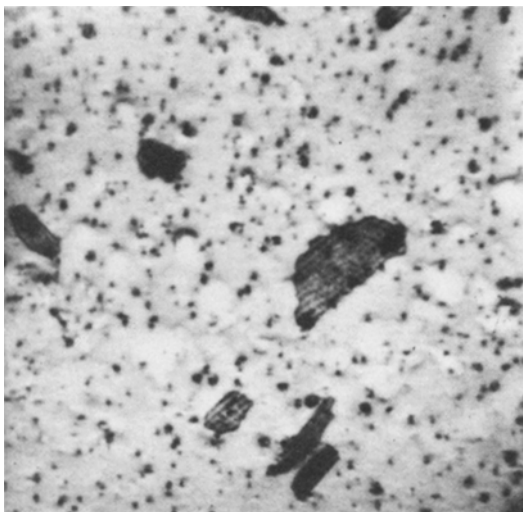


Figure 7 Brine-quenched from the solution treatment temperature and aged at 700° C for 35 h, showing matrix and stacking fault precipitation.  $\times 45\ 000$ .

precipitates after ageing at 700° C, it was believed that matrix precipitates would also form at and above 700° C provided particles nucleated at lower temperatures had grown to a size such that the critical size required for nucleation at 700° C had been attained. To test this suggestion step ageing was carried out by directly ageing to 550° C for 5 and 40h and then up-ageing at 700° C for 70h. The results are shown in Fig. 9. Holding at 500° C for 40h gave a larger density of precipitates than holding at the same temperature

TABLE III Density of matrix precipitates (detected from strain contrast) after various quenching and ageing procedures

Ageing condition	Density $\text{cm}^{-3}$
Water quenched and aged	
650° C for 40 h	$1.1 \times 10^{12}$
650° C for 80 h	$6.4 \times 10^{15}$
680° C for 72 h	$3.2 \times 10^{15}$
700° C for 40 h	$2.1 \times 10^{10}$
Directly aged	
680° C for 70 h	$1.1 \times 10^{15}$
550° C (5 h) secondary aged at 700° C (70 h)	$2.5 \times 10^{14}$
550° C (40 h) secondary aged at 700° C (70 h)	$3.1 \times 10^{14}$

for 5h before the treatment at 700° C, see Table III.

### 3.2.6. Examination of deformed and aged samples

Such samples had to be prepared from bulk specimens; hence, it was necessary to mechanically polish prior to the final electropolishing treatment. As a result of the mechanical preparation stage large twins were formed throughout the matrix; these structural features made the interpretation of precipitation evidence difficult.

## 4. Discussion

These experiments show that a high density of vanadium carbide precipitates form in this medium carbon steel in the temperature range 550 to 700° C. At the lower end of this range, i.e. where

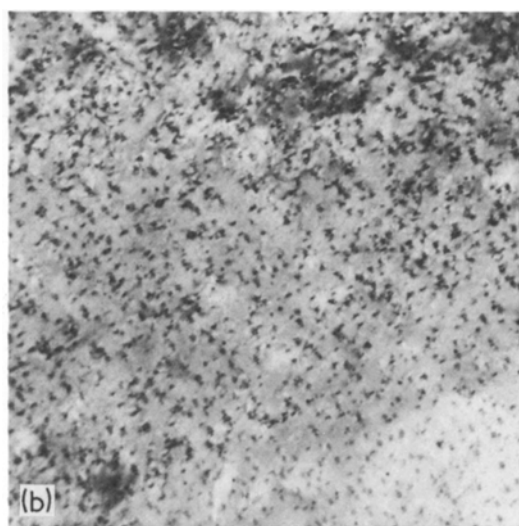
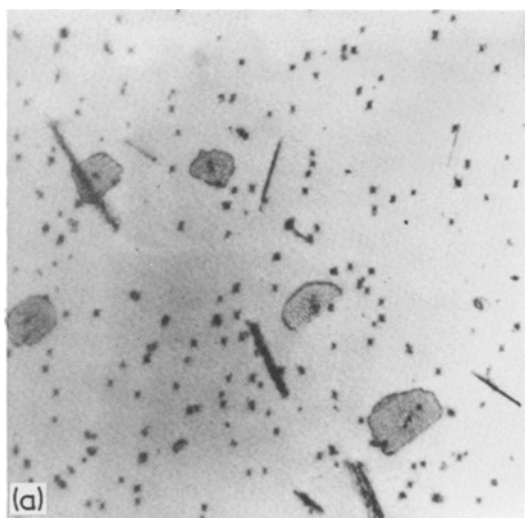


Figure 8 Mn–V–C steel aged at 680° C for 70 h after (a) direct ageing from solution-treatment temperature – matrix and stacking fault precipitation present, (b) solution-treatment and brine-quenching – showing matrix precipitation only;  $\times 45\ 000$ .

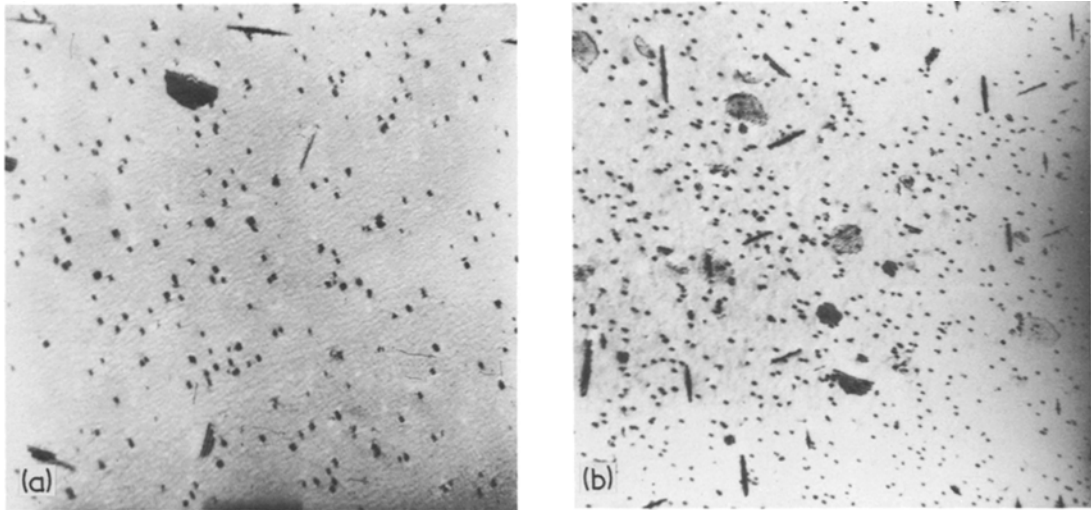


Figure 9 Samples that have been directly quenched from the solution-treatment temperature to 550° C and held for (a) 5 h and (b) 40 h and then subjected to a secondary ageing treatment at 700° C.  $\times 27\,000$ .

the ausforming process takes place, a long incubation period for the precipitate reaction of  $\sim 30$ h exists. Such a long “period” would suggest that the reaction is of little consequence to an understanding of the thermo-mechanical treatment. However, the observation that plastic deformation appreciably reduces the incubation time restores the possibility of direct involvement. Before examining this possibility further it is necessary to examine the precipitate reaction results in more detail.

The observation of matrix and stacking fault precipitation has been made by earlier workers [6–8] on chromium–nickel austenite steels with strong carbide forming elements, vanadium, tantalum, etc, present. The steel examined in the present work possessed a much lower carbide forming element to carbon ratio than had previously been studied. Thus it can be seen that precipitate densities of  $\sim 10^{16} \text{ cm}^{-3}$  can be obtained in steels with V:C ratios only one third of that worked on hitherto [9].

#### 4.1. Nucleation of matrix precipitates

Electrical resistance measurements have shown that during isothermal ageing of solution-treated and water-quenched material an incubation period exists, i.e. 7h at 675° C, 19h at 650° C, and 57h at 550° C. The first clear evidence of precipitation at 650° C as witnessed by electron microscopy, was after ageing the sample for 40h. Prior to this stage there was some evidence of an extremely

fine structure in the matrix whilst the incidence of vacancy loops was minimal. This evidence gives support to a nucleation mechanism that begins with the prior formation of solute-vacancy clusters and not one involving collapsed vacancy loops. It may be that vacancies retained by fast quenching rates from the solution treatment temperature associate with the relatively large vanadium atoms. The resultant “solute-vacancy pairs” could be sufficiently mobile to slowly form clusters on a local basis. Further indirect evidence of this behaviour comes from two sources. In the first place a step ageing experiment which showed that quenching from solution treatment temperature down to 550° C holding for 5 and 40h increases the precipitate density when aged at 700° C. Both the holding times at 550° C were within the incubation period given by the electrical resistance–time plots. Mechanical behaviour [11] of this steel at 550° C is the second indication. Serrated stress–strain curves result at appropriate strain-rates in situations where precipitation is not evident.

It would seem that solute depletion in the accepted sense does not occur during the observed “incubation period”, but the growth of clusters into stable nuclei takes place by local migration of vanadium-vacancy groupings. As to whether carbon atoms play any role in this mechanism is difficult to forecast. However, a significant local vacancy concentration may be required before effective stable carbides are formed. The strain

lobes accompanying the carbides at early stages of growth indicate that large transformation strains are associated with their formation and add support to this mechanism.

#### 4.2. Growth of matrix precipitates

A continuous decrease in electrical resistance takes place at each of the ageing temperatures once the incubation time has passed. Electron microscopy work showed that the number of precipitates increased from  $10^{12}$  to  $10^{15}$   $\text{cm}^{-3}$  as length of the ageing period at  $650^\circ\text{C}$  changed from 40 to 80 h, i.e. from 0.04 to 0.12 fraction transformed. These observations tend to imply that nucleation is continuing simultaneously with growth. Analysis of electrical resistance–time plots using the Johnson–Mehl equation shows that the time exponent  $n = 1.8$  for  $y < 0.1$ . Such values have been interpreted [10] as resulting from a decreasing nucleation rate accompanied by diffusional growth. At  $y > 0.1$  the  $n$  value changes to 1.1 for the remainder of the reaction implying zero nucleation rate and transformation proceeding simply by growth. These observations differ from those of Silcock [9] who measured  $n$  values using a dilatometer technique for higher vanadium–carbon ratio steels; Silcock obtained  $n$  values greater than 2 thus indicating continuing nucleation throughout the reaction. Hence, the electron microscope evidence in this and previously published work [9] can be explained if it is assumed that a size distribution of “clusters” is produced during the incubation period and this persists during the initial nucleation and growth processes.

The step ageing experiments from  $550$  to  $700^\circ\text{C}$  performed in the present investigation help confirm the above reasoning. This would suggest that there is smooth growth process from clusters through stable nuclei to precipitates observed with strain contrast, providing a certain critical ageing temperature has not been exceeded. Above this critical temperature the clusters will have to reach a stable size before further growth occurs, i.e. the length of pretreatment at  $550^\circ\text{C}$  (limited by the incubation period) effectively controls the number of stable nuclei at  $700^\circ\text{C}$ .

#### 4.3. Stacking fault precipitation

In the brine quenched samples stacking fault precipitation was observed when aged above  $700^\circ\text{C}$ , along with those in the matrix, whereas in directly

aged specimens stacking fault precipitation was formed over a wide temperature range. In the directly aged samples the number of vacancy–solute atom clusters of a size that allowed them to stabilize and become effective matrix precipitate nuclei may be less. This can mean that a sufficient concentration of solute (vanadium) atoms were not associated with critical sized clusters and hence, they could participate in stacking fault formation. Previous work [5] has shown that stacking fault formation was dependent on supersaturation of solute atoms as well as dislocation density and concentration of vacancies. In the case of the water-quenched and aged samples the incidence of critical sized clusters again may become smaller as the ageing temperature is raised, thus providing the opportunity for the nucleation of precipitates on dislocations. Once fault growth has begun then the production of vacancies by climb of the Frank partials helps accommodate carbide precipitates at least while they are in the nucleation and early growth stages.

Johnson–Mehl analysis of the electrical resistance data obtained on the brine-quenched and aged material indicates that the exponent  $n$  increases from 1.8 to 2.2 for  $y < 0.1$  as the ageing temperature increases to  $700^\circ\text{C}$ . The higher values could possibly take some account of stacking fault precipitation, which previous kinetic work [5] on niobium–low carbon steels has shown to occur with  $n > 2.5$ , i.e. high values are associated with an increasing nucleation rate particularly at early stages of fault formation. Obviously such values have not been recognized in the current case because of the low “ $n$ ” values of the matrix precipitate process which is taking place at the same time.

From the evidence accumulated here there appears to be direct competition between stacking fault and matrix precipitation. Matrix precipitation is favoured by low ageing temperatures, intermediate holding at lower temperatures, i.e. below  $650^\circ\text{C}$ . Obviously solute concentration is an important consideration, at higher concentrations of carbide forming solute greater incidence of stacking fault precipitation may be in evidence at lower temperatures, particularly in austenites of low stacking fault energy. From earlier work it is evident that long incubation periods are necessary for nucleation of stacking fault precipitates. Hence, at the end of the incubation period at a particular ageing temperature the



stable cluster growth has reduced the available solute concentration below the critical level required for fault nucleation then the latter type of precipitation does not take place. Once fault precipitation has begun and sufficient solute concentration is still available then precipitation may advance more swiftly by this mechanism. Also the generation of vacancies by the climb of Frank partials considerably reduces the strain fields around carbide precipitates.

#### 4.4. Effect of deformation

Electron microscope work has not been carried out on deformed and aged samples due to difficulties in preparing foils; thus detailed investigations on the morphology of precipitates could not be made. Nevertheless, the electrical resistance-time data obtained on such samples did provide some useful information. It is clear that increasing amounts of deformation significantly decreases the incubation period for precipitation, e.g. 7 to 0.7h at 675°C with 10% deformation as well as accelerating the overall reaction. Further, the total resistance drop at reaction completion decreased with increasing deformation.

The imposition of deformation may influence the kinetics by introducing dislocations which interact with vacancy-solute clusters. Support for this comes from some mechanical tensile tests (reported elsewhere [11]) that have been carried out on these alloys in the appropriate temperature range providing clear evidence of serrated stress-strain curves which may be interpreted as resulting from dislocation-cluster interaction. Hence, effective cluster growth may actually take place during deformation, i.e. dislocations moving along collecting such entities until they become locked. Thus early formation of stable nuclei could take place on dislocations reducing the observed incubation period. The Johnson-Mehl "n" values indicate the same trends as for the straight aged data, i.e. decreasing nucleating rate up to  $y < 0.1$  followed by diffusional growth of a static distribution of precipitates.

The total drop of electrical resistance on ageing will depend on the number of clusters and solute atoms available in the matrix for precipitate growth. In the deformed and aged case a significant number of clusters were already segregated on dislocations and as such may be regarded as being removed from solution, thus leaving a "reduced matrix solute content". It may also be

relevant to add that as a result of dislocation-cluster interaction any strain fields associated with such species may be reduced in intensity, thus permitting further growth.

#### 4.5. Ausforming response

It is clear that deformation does alter carbide precipitation kinetics. However, it is not necessarily the presence of precipitates at sizes which can be resolved by an electron microscope, i.e.  $>40 \text{ \AA}$  which are relevant to the ausforming process as suggested by Thomas *et al.* [3]. The most important interaction is likely to be that between solute-vacancy clusters and dislocations. In these circumstances dislocation locking and multiplication may be the controlling factors. Thus matrices that are capable of being deformed to produce large densities of well distributed dislocations may be the most responsive to ausforming.

#### 5. Conclusions

(1) The precipitation of vanadium carbides in the matrix is diffusion controlled and the process has an activation energy of  $295 \text{ kJ mol}^{-1}$ , which is close to values associated with diffusion solute atoms like vanadium in iron.

(2) Electrical resistance measurements and electron microscope observations on brine quenched specimens show that matrix precipitation occurs in this low vanadium-medium carbon steel in the temperature range 550 to 700°C, with precipitate densities close to  $10^{16} \text{ cm}^{-3}$ .

(3) Long incubation periods prior to effective precipitate growth occurred at all temperatures, e.g. 19h at 650°C. Analysis of the reaction curves suggested that the nucleation rate decreases after the incubation period to effectively zero at 0.1 fraction transformed.

(4) Direct ageing experiments, i.e. solution treatment direct to ageing without intermediate cool to room temperature showed that matrix precipitation under such conditions did not occur above 700°C. Carbide precipitation on stacking faults and undissociated dislocations occurred instead.

(5) Higher densities of matrix precipitates were observed in samples that had been step quenched to an intermediate temperature, e.g. 550°C, prior to a final ageing treatment at 700°C (i.e. in comparison to directly aged samples at 700°C).

(6) Prior deformation at the ageing temperature speeds up the whole reaction, e.g. 10% deforma-

tion decreases the incubation period by an order of magnitude.

(7) It is maintained that stable nuclei of precipitates are produced by the migration and growth of solute atom-vacancy clusters.

(8) The imposition of heavy deformation on "metastable" austenites in low alloy steels may cause dislocation-cluster interaction which may help produce high densities of dislocations evenly spread throughout the matrix. Such a mechanism could provide a major strengthening contribution to a steel which is said to possess a strong response to ausforming.

### Acknowledgements

The authors would like to extend their thanks to Dr B. Noble for helpful guidance on the electron microscopic aspects of this work, and Mr C. Oxlee of R.A.R.D.E. Fort Halstead, for providing the manganese-vanadium steels. One of the authors (NRN) is grateful to the Ministry of Defence for providing a research grant whilst this programme was carried out. Also our thanks are extended to Professor J.S.L. Leach for the provision of laboratory facilities.

### References

1. L. RAYMOND, W. W. GERBERICH and C. F. MARTIN, Proceedings of the 2nd International Symposium on High Strength Materials, Berkeley (Wiley, New York, 1965) p. 297.
2. R. PHILLIPS and W. E. DUCKWORTH, *ibid*, p. 307.
3. G. THOMAS, D. SCHMATZ and W. W. GERBERICH, *ibid*, p. 251.
4. W. JUSTUSSON and D. SCHMATZ, *Trans. Amer. Soc. Metals* **35** (1962) 640.
5. S. J. HARRIS and N. R. NAG, *J. Mater. Sci.* **10** (1975) 1137.
6. J. J. IRANI and R. T. WEINER, *J. Iron Steel Institute* **203** (1965) 913.
7. J. M. SILCOCK and A. W. DENHAM, in "Mechanism of Phase Transformations in Crystalline Solids", (Institute of Metals Monograph No. 33, London, 1969) p. 59.
8. F. H. FROES and D. H. WARRINGTON, *Trans. Met. Soc. AIME* **245** (1969) 2009.
9. J. M. SILCOCK, *J. Iron Steel Institute* **211** (1973) 792.
10. J. M. CHRISTIAN, "Theory of transformations in metals and alloys" (Pergamon Press, Oxford, 1965).
11. S. J. HARRIS and N. R. NAG, to be published.

Received 28 October 1975 and accepted 19 January 1976.